Fluorinated Polymer Films from Acylation of ATRP Surface-Initiated Poly(hydroxyethyl methacrylate)

Eric L. Brantley and G. Kane Jennings*

Department of Chemical Engineering, Vanderbilt University, Nashville, Tennessee 37235

Received September 29, 2003; Revised Manuscript Received December 10, 2003

ABSTRACT: We report a new strategy to prepare partially fluorinated polymer films by utilizing surface-initiated films of poly(2-hydroxyethyl methacrylate) (PHEMA) grown onto gold surfaces via atom transfer radical polymerization (ATRP). Hydroxyl side chains of PHEMA were reacted with perfluoroalkyl (C3F7 and C7F15) and perfluoroaryl (C6F5) acid chlorides to yield partially fluorinated surface-initiated polymer films with conversions ranging from ∼70 to 85%. The resulting fluorinated PHEMA films dramatically altered surface and barrier properties, particularly lowering the critical surface tension to as low as 9 mN/m and boosting film resistance by as much as 5 orders of magnitude compared to that of PHEMA. Film properties depend on the chemical composition and length of the fluorinated side chains. The longer C7F15 fluoroalkyl chain structured the film to a greater extent than the shorter C3F7 chain and yielded improved barrier properties and lower critical surface tension. The C7F15 groups are oriented nearly normal to the surface at the air−film interface and predominantly parallel to the surface in the bulk. Modification of PHEMA with the fluoroaryl side chain produced the best barrier properties of the three side chains investigated.

Introduction

Fluorinated polymer films exhibit excellent barrier properties[1] and extremely low critical surface tensions,[2] causing water and oils to bead up on exposure. Methods commonly used to deposit fluorinated polymers onto a surface include spin-coating,[3] solution-casting,[4] and chemical adsorption.[5] These methods produce films with the properties of fluorinated polymers but often in a relatively uncontrolled fashion. While chemical adsorption produces only polymer monolayers,[5] spin-coating and solution-casting exhibit poor control over film thickness in the submicron range and produce films that are only physically attached to the underlying substrate.[3,4] Plasma deposition[6] and chemical vapor deposition[7] can provide greater control over film thickness by growing the fluorinated films from an underlying surface, but these methods require low pressure and specialized equipment and often yield films with compositions that are not well-defined.[6,7] In general, high cost and difficult processability limit the use of fluorinated polymers in many applications.[3,8−10]

One route to fluorinated polymer films that has not been fully explored is surface-initiated polymerization. The advantages of growing a film directly from a surface include well-controlled growth, especially when the kinetics exhibit living character,[11] and stability due to covalent attachment of the polymer backbone to the surface.[12,13] Jung et al.[8] have prepared surface-initiated films on porous silica from hydrophobic fluoromonomers using a radical-chain polymerization. The films exhibited highly hydrophobic and oleophobic surfaces, but the film growth was somewhat slow, producing only 70 nm films after 27 h exposures at 60 °C.[8] The ability to prepare surface-initiated, partially fluorinated films over a much greater range of thicknesses—from ultrathin films used to modify surface properties to thicker films that are ideal as protective coatings—could greatly impact the applications of these films.

One such surface-initiated polymerization technique that allows a high level of control over film growth is atom transfer radical polymerization (ATRP).[9,14−24] ATRP in solution has been performed extensively on numerous vinyl monomers with recently increasing focus on growing films from a surface. When ATRP was originally applied to the surface-initiated case, polymerization kinetics was slowed tremendously due to an increase in termination reactions.[14,17] Recent efforts to increase surface-initiated growth rates have relied on innovations in solution-phase ATRP. For example, Armes and co-workers have shown[18−21] that ATRP of hydrophilic monomers in aqueous media at room temperature accelerates solution-phase polymer growth. Bruening, Baker, and co-workers[22] have remarkably and successfully extended this strategy to prepare surface-initiated films of poly(2-hydroxyethyl methacrylate) (PHEMA) with controlled thicknesses of up to 700 nm. They also demonstrated the ability to derivatize the reactive hydroxyl side chains of PHEMA after film growth using low-molecular-weight hydrocarbon acid chlorides in an acylation reaction. The method of Bruening, Baker, and co-workers[22] provides insight toward an alternative strategy for preparing partially fluorinated polymer films. While the solution-phase ATRP of hydrophobic fluoromonomers exhibits rather sluggish kinetics,[9] partially fluorinated polymer films could be prepared by acylation of hydroxyl side chains of surface-initiated PHEMA with fluorinated acid chlorides. Such a strategy would provide a test bed to determine the role of side chain composition on film and surface properties by using various acid chlorides to modify the same base film (PHEMA).

We report herein the use of surface-initiated PHEMA films as supports with reactive side chains to enable attachment of fluorocarbon groups by acylation with a fluorinated acid chloride, including heptafluorobutyryl chloride (C_3F_7COCl), pentadecafluorooctanoyl chloride

* To whom correspondence should be addressed. E-mail: jenningk@vuse.vanderbilt.edu.

10.1021/ma035471v CCC: $27.50
Published on Web 01/22/2004

Scheme 1. Acylation of PHEMA with Fluorinated Acid Chlorides

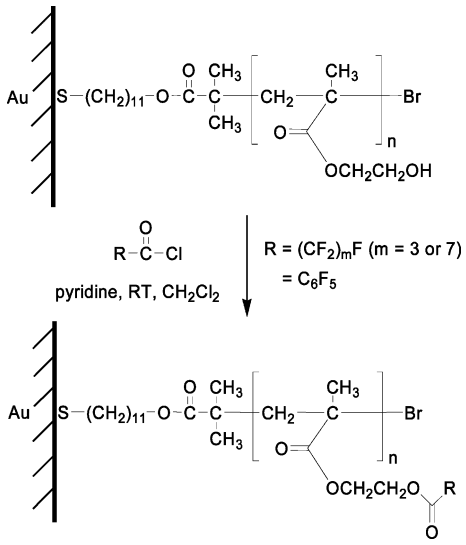

($C_7F_{15}COCl$), and pentafluorobenzoyl chloride (C_6F_5-COCl) (Scheme 1). This approach to partially fluorinated polymer films exploits the rapid kinetics, precise control, and covalent attachment of surface-initiated PHEMA growth, and the fluorination is performed directly on the surface-attached film for ease of processing and separations. Reihs and co-workers[25,26] have demonstrated the ability to use fluorinated acid chlorides to acylate hydroxyl side chains of polymers in solution, originally working with hydroborated polystyrene-*block*-polyisoprene and more recently poly(methyl methacrylate)-*block*-poly(2-hydroxyethyl methacrylate). Their work involved block copolymers without using surface-initiated polymerization methods and did not extensively focus on the modification of surface properties. This paper addresses important questions of whether modification of the side chains of an existing film with fluorocarbon groups is sufficient to achieve the properties of fluorocarbon films and how the length and chemical nature of the fluorinated side chain affect film and surface properties. Our work combines complementary characterization methods to determine the role of fluorination on film composition and structure, thickness, barrier properties, and surface wettability.

Experimental Section

Materials. CuCl (99.995+%), $CuBr_2$ (99.999%), 2,2′-bipyridine (bpy, 99+%), 2-hydroxyethyl methacrylate (HEMA, >99%), pyridine (99+%), heptafluorobutyryl chloride (C_3F_7COCl, 98%), pentadecafluorooctanoyl chloride ($C_7F_{15}COCl$, 97%), pentafluorobenzoyl chloride (C_6F_5COCl, 99%), $K_3Fe(CN)_6$ (99+%), $K_4Fe(CN)_6 \cdot 3H_2O$ (99%), KOH (85+%), and hexadecane (99%) were used as received from Aldrich. *N*,*N*-Dimethylformamide (DMF, 99.9%), dichloromethane (99.9%), Na_2SO_4 (anhydrous), *n*-hexane (99.9%), *n*-octane (99%), *n*-decane (99+%), *n*-dodecane (99%), and *n*-tetradecane (99+%) were used as received from Fisher. Gold shot (99.99%) and chromium-coated tungsten filaments were obtained from J&J Materials and R.D. Mathis, respectively. Silicon (100) wafers (Montco Silicon) were rinsed with ethanol and deionized water and dried with nitrogen. Ethanol (AAPER, absolute) was used as received. NaCl coverslips (International Crystal Labs) were used as received. Deionized water (16.7 MΩ·cm) was purified with a Modu-Pure system and used as a solvent during polymerization and for rinsing. An initiator-terminated disulfide, $(BrC(CH_3)_2COO(CH_2)_{11}S)_2$, was synthesized as described in the literature.[23]

Preparation of Gold Substrates. Gold substrates were prepared by evaporating chromium (100 Å) and gold (1250 Å) in sequence onto silicon (100) wafers at rates of 1−2 Å s^{-1} in a diffusion-pumped chamber with a base pressure of 4×10^{-6} Torr. After removal from the evaporation chamber, the wafers were typically cut into 1 cm × 3 cm pieces.

Polymerization. Procedures followed to make PHEMA films via water-accelerated ATRP are similar to those outlined in Huang et al.[22] Gold substrates were first placed in a 1 mM ethanol solution of $(BrC(CH_3)_2COO(CH_2)_{11}S)_2$ for 24 h. The initiated samples were then rinsed with ethanol, dried with nitrogen, and placed in vials that were subsequently degassed and back-filled with nitrogen. A Cu^I/Cu^{II}/bpy (69 mM CuCl, 20 mM $CuBr_2$, 195 mM bpy) system in a 50:50 v:v water/HEMA solution[22] was used for polymerization. Since a glovebox was not available and oxygen will oxidize the activating Cu^I species and terminate polymerization, the mixture was placed in a Schlenk flask sealed with a rubber septum and was degassed by performing three freeze−pump−thaw cycles. This was followed by transfer of the solution via cannula into vials containing up to six samples each. After polymerizing for 12 h at room temperature, the samples were thoroughly rinsed with water and DMF and then dried with nitrogen. As measured by ellipsometry with samples from seven different batches, PHEMA film thicknesses were 270 ± 20 nm under these conditions.

Fluorination. Gold surfaces with PHEMA films were exposed to 80 mM solutions of heptafluorobutyryl chloride (C_3F_7COCl), pentadecafluorooctanoyl chloride ($C_7F_{15}COCl$), or pentafluorobenzoyl chloride (C_6F_5COCl) with 100 mM pyridine in dichloromethane for 24 h to give PHEMA films with mostly fluorinated side chains (Scheme 1). The acylation time could be reduced from 24 to 1 h without an observable change in the composition of the films as determined by reflectance−absorption infrared spectroscopy. After reaction, the films were rinsed with dichloromethane and dried with nitrogen.

Characterization Methods. Polymer film properties were evaluated using the following methods before acylation to provide a baseline measurement and once again after acylation to track changes in film properties. Reflectance−absorption infrared spectroscopy (RAIRS) was performed using a Bio-Rad Excalibur FTS-3000 infrared spectrometer. The p-polarized light was incident at 80° from the surface normal. The instrument was run in single reflection mode and equipped with a Universal sampling accessory. A liquid nitrogen-cooled, narrow-band MCT detector was used to detect reflected light. Spectral resolution was 2 cm^{-1} after triangular apodization. Each spectrum was accumulated over 1000 scans with a deuterated octadecanethiol-d_{37} self-assembled monolayer on gold as the background. To allow comparison between the orientation of fluorinated acid chlorides in the liquid phase and fluorinated species within the film, transmission IR spectra were obtained for the pure liquid acid chlorides confined between two NaCl coverslips. Spectra were accumulated over 1000 scans using a NaCl plate as background.

Ellipsometry measurements were taken on a J.A. Woollam Co. M-2000DI variable angle spectroscopic ellipsometer with WVASE32 software for modeling. Measurements at three spots per sample were taken with light incident at a 75° angle from the surface normal using wavelengths from 250 to 1000 nm with the refractive index assumed to be 1.5 at all wavelengths. While 1.5 is higher than the index of refraction for purely fluorocarbon films (1.37),[27] use of values less than 1.5 yielded inferior fits to the data by the modeling software. Optical constants of a bare gold sample were determined by ellipsometry and used as the baseline from which all polymer film samples were measured. Film thickness of the polymer layer present on samples, regardless of modification, was fit to a Cauchy layer model setting the refractive index to 1.5.

A Rame-Hart manual contact angle goniometer with a microliter syringe was used to measure advancing and receding contact angles on static drops of water and hexadecane on the polymer surfaces. The needle tip of the syringe remained inside the liquid drop while measurements were taken on both sides of ~5 μL drops. Reported values and ranges represent

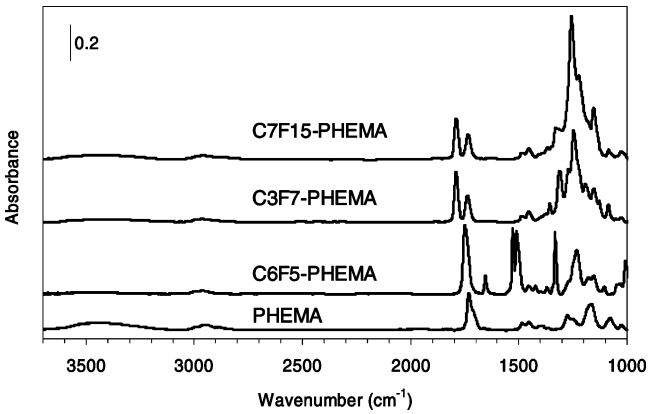

Figure 1. Reflectance−absorption IR spectra of PHEMA films on gold before and after exposure to fluorinated acid chlorides. There are several key regions of interest when evaluating effectiveness of the acylation reaction: C−O and CF_2, 1100−1400 cm^{-1}; C⋯C, 1500−1700 cm^{-1}; C═O, 1700−1800 cm^{-1}; OH, 3100−3700 cm^{-1}.

the average and standard deviation of values obtained for eight independent sample preparations.

Electrochemical impedance spectroscopy (EIS) was performed with a Gamry Instruments CMS300 impedance system interfaced to a personal computer. A flat-cell (EG&G Instruments) was used to expose only 1 cm^2 of each sample to the aqueous solution containing electrolyte and redox probes while preventing sample edges from being exposed. The electrochemical cell consisted of an aqueous solution of 1 mM $K_4Fe(CN)_6 \cdot 3H_2O$, 1 mM $K_3Fe(CN)_6$, and 0.1 M Na_2SO_4 with a Ag/AgCl/saturated KCl reference electrode, a gold substrate counter electrode, and a gold substrate containing the film to be studied as the working electrode. All data were collected in the range from 10^{-1} to 10^4 Hz using 10 points per decade and were fit with an appropriate equivalent circuit (vide infra) to determine resistance and capacitance values. Reported values and ranges for resistance and capacitance represent the averages and standard deviations of values obtained from at least four independent sample preparations.

Results and Discussion

Film Composition and Structure. We used RAIRS to monitor compositional changes within the polymer films due to acylation by C_3F_7COCl, $C_7F_{15}COCl$, or C_6F_5COCl. Figure 1 shows the IR spectra of PHEMA along with all three types of fluorinated PHEMA, referred to as C3F7-PHEMA, C7F15-PHEMA, and C6F5-PHEMA. The most readily quantifiable change in the spectra that is indicative of successful acylation is diminution of the hydroxyl peak in the region from 3100 to 3700 cm^{-1}, as the hydroxyl side chains of PHEMA are converted to fluorinated esters. We have used this diminution of integrated hydroxyl peak area (A_{OH}) to estimate conversion (χ) of the hydroxyl side chains as

$$\chi = 1 - \frac{A_{\text{OH, fluorinated PHEMA}}}{A_{\text{OH, PHEMA}}} \qquad (1)$$

which assumes that any change in integrated hydroxyl peak area is due solely to acylation and not to orientational changes of the unreacted hydroxyl groups. Because of the distinct differences in perfluorinated chain length and type, some differences in conversion for the acid chlorides were expected. However, since such a high concentration and long time were used, we observed no significant difference in conversion between the two fluoroalkyl chains: 70 ± 4% for C3F7-PHEMA and 67 ± 10% for C7F15-PHEMA. This similar conversion for different fluoroalkyl lengths suggests that transport of the acid chloride into the film does not limit the ultimate conversion but that steric effects due to the packing of adjacent fluorocarbon chains along a common backbone may play a role. A higher conversion of 83 ± 4% was observed for C6F5-PHEMA. We attribute the higher conversion to $\pi-\pi$ stacking of the perfluoroaryl groups, which would result in a lower packing parameter based on the face-to-face distance between the disklike perfluoroaryl groups[28] (3.2 Å) vs that for perfluoroalkyl chains[5] (5.6 Å) and allow greater accessibility to unreacted hydroxyl groups along a common backbone.

Further analysis of Figure 1 reveals key differences between the spectra of the fluoroalkyl- and fluoroaryl-modified PHEMA and unmodified PHEMA in the region of 1100−1800 cm^{-1}. Every repeat unit of the PHEMA film has an ester immediately off the main backbone chain, and the associated carbonyl appears in the IR spectrum at 1733 cm^{-1}. Also, because of the presence of hydroxyl groups throughout the PHEMA film that can hydrogen bond with this carbonyl, a shoulder appears on the carbonyl peak that causes it to broaden toward lower wavenumbers.[29,30] Acylation greatly reduces hydrogen bonding within the film, which diminishes the shoulder on the original carbonyl peak and causes an apparent shift to higher wavenumbers (1735 cm^{-1} for C7F15-PHEMA and to 1737 cm^{-1} for C3F7-PHEMA). Acylation also produces another ester along the side chain, which results in the appearance of a second carbonyl peak in the spectrum. For films with fluoroalkyl side chains, this new carbonyl peak appears at significantly higher wavenumbers (∼1790 cm^{-1}) due to α-halogen substitution.[31] For C6F5-PHEMA, the new carbonyl peak combines with the original one to yield a broad peak at ∼1749 cm^{-1}. While α-halogen substitution is absent in this case, the fluorine atoms on the aromatic ring are electron-withdrawing groups, thus raising the carbonyl peak frequency, but conjugation of the carbonyl with the nearby aromatic ring likely offsets this effect and lowers the frequency[31] in comparison to the perfluoroalkyl-substituted PHEMA. The overall result of these competing effects is observed.

Careful examination of Figure 1 reveals that the PHEMA carbonyl peak loses ∼30% intensity upon acylation with C_3F_7COCl or $C_7F_{15}COCl$. This reduction is most likely due to film expansion, which alters the orientation of the carbonyl and thus its intensity in the IR spectrum. This explanation is supported by the fact that hydrolysis of the fluorinated esters (vide infra) returns the PHEMA carbonyl to its original intensity. As fluorocarbon groups are added to the side chain, the surface-attached polymer chain (backbone plus side chains) requires additional space and likely expands to orient more normal to the surface, thus altering the orientation of the original carbonyl groups.

Introduction of fluorinated side chains to the polymer film is also evidenced by the appearance of large peaks throughout the region from 1100 to 1400 cm^{-1}. Since fluoroalkyl chains exhibit a helical structure, there are two types of CF_2 stretching peaks expected in the IR: those lying along the helical axis ($\nu_{ax}^{CF_2}$, 1300−1400 cm^{-1}) and those perpendicular to the helical axis ($\nu_{pd}^{CF_2}$, 1100−1300 cm^{-1}).[5,32] The ratio of $\nu_{pd}^{CF_2}$ to $\nu_{ax}^{CF_2}$ absorbance for the film, relative to the same ratio for an isotropic orientation of the acid chlorides in the liquid state, provides information on the orientation of the fluorocarbon side chains in the polymer film relative to

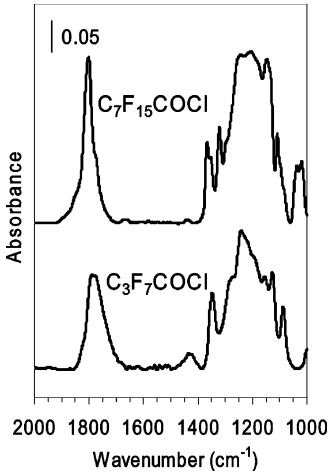

Figure 2. Transmission IR spectra of perfluoroalkyl acid chlorides in the liquid state. The relative intensity of axial (1300−1400 cm^{-1}) and perpendicular (1100−1300 cm^{-1}) CF_2 peaks in the pure liquids provides a reference to assess orientation of fluorinated side chains in the polymer films.

the surface normal. Given the surface selection rules in RAIRS,[33] the intensity for a given mode in the IR spectrum is proportional to the square of the component of its dynamic dipole moment oriented along the surface normal. Hence, when the ratio of $\nu_{pd}^{CF_2}$ to $\nu_{ax}^{CF_2}$ is greater in the film than in the isotropic liquid, the fluorocarbon helical axis generally lies more along the parallel to the substrate surface, but when this ratio is less in the film than in the isotropic liquid, the fluorocarbon helical axis is more normal to the surface.[5] Transmission IR spectra of the randomly oriented liquid fluoroalkyl acid chlorides (Figure 2) yield a $\nu_{pd}^{CF_2}$:$\nu_{ax}^{CF_2}$ absorbance ratio of ∼1.8. Clearly for the bulk liquid, $\nu_{pd}^{CF_2}$ are more readily observed than $\nu_{ax}^{CF_2}$ even when chains are randomly oriented. For C3F7-PHEMA (Figure 1), the $\nu_{pd}^{CF_2}$:$\nu_{ax}^{CF_2}$ absorbance ratio is also ∼1.8, which suggests that these chains are randomly oriented within the film in similar fashion as the pure acid chloride. C7F15-PHEMA has a much higher $\nu_{pd}^{CF_2}$:$\nu_{ax}^{CF_2}$ absorbance ratio (∼4.5), indicating that the C7F15 side chains in the polymer film are aligned more parallel to the metal surface such that the axial CF_2 peaks are nearly undetected. Most likely, the C7F15 side chains align within the film to maximize interchain van der Waals interactions, whereas C3F7 side chains are too short to promote such structuring and thereby assume more random orientations.

The fluorobenzoyl side chain also shows activity in the C−F region, but it cannot form a helical structure and has no CF_2 stretching so the observations for this sample are completely different. The aromatic C−F stretch shows two peaks between 1200 and 1350 cm^{-1}, but there is no good indicator from IR of how these aromatic side chains are oriented within the film. Other evidence for the addition of the fluorobenzoyl group to the side chain is the presence of peaks for fluorinated C⋯C aromatic ring stretching from 1500 to 1700 cm^{-1}.[6,34]

Film Thickness. Table 1 shows fluorinated film thicknesses obtained by ellipsometry before and after acylation. The water-accelerated ATRP of PHEMA resulted in 270 nm thick films after 12 h. PHEMA is envisioned as being loosely packed, but the addition of fluorocarbon side chains would still cause an expansion of the film to minimize constraints. After fluorination, the greatest thickness increase over that of PHEMA was observed for C7F15-PHEMA followed by C6F5-PHEMA and then C3F7-PHEMA. From the observed changes, a longer side chain requires more space and thus increases film thickness by inducing an extension of the PHEMA backbone to a greater extent than a shorter side chain would.

Table 1. Thickness Change of PHEMA Films upon Acylation with Fluorinated Acid Chlorides[a]

side chain	thickness (nm) before	thickness (nm) after	obsd increase (%)	theor increase (MW) (%)	theor increase (vol) (%)
C3F7	277	373	35	106	58
C6F5	273	452	65	124	47
C7F15	275	483	76	204	105

[a] Thickness increase observed for thinner PHEMA films (50−200 nm) tend to be in much closer agreement with the volume-predicted values. The observed average increase for these films from six preparations was 60% for C3F7, 45% for C6F5, and 115% for C7F15.

Expected thickness increases after addition of side chains were estimated using two separate methods while also accounting for conversion. Predictions based solely on the increase in molecular weight of the repeat unit upon acylation have been used for addition of hydrocarbon chains to films.[22] On the basis of this model, the trend in thickness for the fluorinated groups is correct, but the actual thickness increases are not nearly as high as predicted (Table 1). We developed another model that is based on the increase in molecular volume of the repeat unit using bond lengths[35,36] and chain packing data[5,28] from the literature. To estimate volumes of the different components in the film, we modeled the fluoroalkyl groups as cylinders with length of 1.3 Å per $-CF_2-$ group[35] and diameter of 5.6 Å based on chain packing data.[5] The fluoroaryl group was modeled as a disk with diameter of 5.0 Å (estimated from the benzene carbon−carbon cross-ring length of 2.8 Å[36] in addition to two C−F lengths of 1.1 Å[35] each) and a thickness of 3.2 Å based on the crystal interplanar face-to-face packing distance.[28] The remainder of the side chain along with the main polymer backbone ($-CH_2C(CH_3)CO_2(CH_2)_2CO_2-$) was approximated as cylinders behaving as normal hydrocarbon chains (lengths of 1.25 Å per $-CH_2-$ group[35] and diameter of 4.2 Å from chain packing data).[5] Carbonyl and ether bonds were approximated as $-CH_3$ or $-CH_2-$ groups, respectively, due to lack of exact data for these groups in similar compounds. As with the molecular weight prediction, all samples were referenced to the basic PHEMA repeat unit to estimate relative increases in the molecular volume. With the volume-based predictor, the predicted changes are much closer to the experimental values at the expense of the overall trend; the C3F7 side chain is predicted to give a slightly larger increase in film thickness than the C6F5 side chain, which is not observed experimentally. Nonetheless, the volume-based model does provide much closer agreement with experimental values and is highly accurate for thinner PHEMA films (see footnote in Table 1).

Surface Wettability. Advancing and receding contact angles (θ_A and θ_R) of water were measured for all polymer films to determine the relative hydrophobicity of the surface. Table 2 gives average contact angles for the fluorinated films along with the values for PHEMA and the bromine-terminated initiator monolayer for comparison. The advancing contact angle of water on

Table 2. Water and Hexadecane Advancing and Receding Contact Angles (deg) for Films on Gold

	water		hexadecane	
sample	θ_A	θ_R	θ_A	θ_R
disulfide initiator	80 ± 2	74 ± 2	<10	<10
PHEMA	75 ± 3	23 ± 2	<10	<10
C6F5-PHEMA	90 ± 2	69 ± 3	<10	<10
C3F7-PHEMA	110 ± 2	70 ± 9	67 ± 2	54 ± 3
C7F15-PHEMA	128 ± 2	71 ± 5	79 ± 2	64 ± 3

the initiator is 80°, which is identical to that reported for a bromine-terminated monolayer film.[37] The extremely low contact angle hysteresis ($\theta_A - \theta_R = 6°$) for the initiator is indicative of a smooth monolayer film as well. Once PHEMA is grown from the initiator, the advancing contact angle does not change significantly, but the hysteresis becomes quite high, suggesting that the surface of the film becomes rough and/or chemically heterogeneous. Upon acylation with the fluorinated acid chlorides, the advancing contact angles of water increase dramatically, consistent with hydrophobic groups at the outermost surface, with the largest effect being observed for the addition of C7F15 side chains. The contact angle hysteresis remains high for the fluoroalkyl-modified films, so there seems to be no or minimal smoothing of the film due to acylation. The advancing contact angle for C6F5-PHEMA may seem low at first glance but is similar to that for a film prepared from the plasma deposition of perfluorobenzene.[6]

Contact angles of hexadecane were also measured on all polymer films. Compared to water, hexadecane is a more sensitive probe of fluorocarbon groups over hydrocarbon groups.[38] C7F15- and C3F7-PHEMA exhibit advancing hexadecane contact angles of 79° and 67°, respectively. Monolayers exhibiting CF_3 surfaces are known to exhibit hexadecane contact angles from 80° down to 70°, depending on the length of the fluorinated chain.[37] The fact that the fluorinated PHEMA films exhibit contact angles that fall in or near this range while hexadecane wets unmodified PHEMA reveals that fluorocarbon groups dominate the surface of both fluoroalkyl-modified polymers. Furthermore, the high hexadecane contact angle exhibited by C7F15-PHEMA suggests that it consists predominantly of a CF_3 surface where the fluorocarbon surface groups are oriented near the surface normal. Hexadecane completely wets C6F5-PHEMA, but this result is not entirely unexpected for the aromatic side group. Fluoroaromatics, as also evidenced by lower water contact angles, do not generally yield surfaces as hydrophobic or oleophobic as their straight chain counterparts.[39]

Since C3F7- and C7F15-PHEMA are extremely hydrophobic and oleophobic, these films should have low critical surface tensions, γ_C, in which the value will suggest whether $-CF_3$ groups indeed dominate the outermost surface. A surface consisting entirely of $-CF_3$ groups[2] has a γ_C of 6−9 mN/m whereas one consisting entirely of $-CF_2-$ groups, as with poly(tetrafluoroethylene),[40] exhibits a γ_C of ∼18 mN/m. To estimate the critical surface tensions of the films, we used the Zisman method[40,41] and selected a series of *n*-alkanes having even numbers of carbons, from hexane to hexadecane, as contacting liquids. θ_A for each of the liquids was measured, and cos θ_A was plotted against γ_L, the surface tension of the liquid (Figure 3). A straight line fit of the data and extrapolation of the line to cos $\theta_A = 1$ gives γ_C of the film such that a liquid with $\gamma_L < \gamma_C$ will completely wet the surface. From Figure 3, C7F15-PHEMA exhibits a γ_C of 9 mN/m, further indicating that the surface consists mostly of $-CF_3$ groups and that the fluorocarbon groups are oriented near the surface normal at the outermost surface. C3F7-PHEMA exhibits a γ_C of 15 mN/m, which is consistent with a mixture of $-CF_3$ groups and other higher energy groups, most likely $-CF_2-$ or $-CH_2-$, at the outer surface.

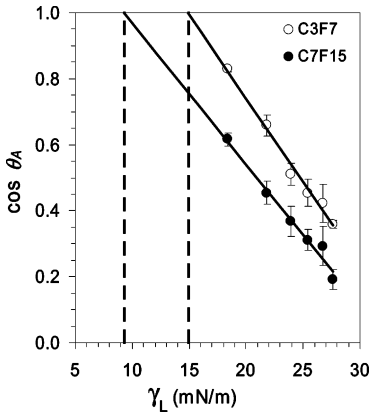

Figure 3. Zisman plot to determine critical surface tension of C3F7- and C7F15-PHEMA. A series of even-numbered *n*-alkanes from hexane to hexadecane was used as contacting liquids. The critical surface tension is 9 mN/m for C7F15-PHEMA and 15 mN/m for C3F7-PHEMA. When an error bar is not observed, the size of the symbol provides an estimate of the error.

A proposed structure of these fluorinated PHEMA films is surmised on the basis of results from wetting measurements and RAIRS. The γ_C values indicate that the C7F15-PHEMA surface consists primarily of $-CF_3$ groups, so the fluorocarbon chains at the surface are mostly normal to the substrate. The dominance of $\nu_{pd}^{CF_2}$ absorbance in the IR, on the other hand, points to the C7F15 chains being oriented more parallel to the substrate in the bulk film. This follows closely with the findings of Genzer and co-workers[42] for spun-cast isoprene polymers with semifluorinated ether side chains. They observed that the fluorinated groups oriented parallel to the surface in the bulk but more normal to the surface at the outer layers. From wettability data, the shorter C3F7 chain is unable to orient at the surface like C7F15 does, and other groups besides $-CF_3$ are present at the outer film layer. The presence of stronger $\nu_{ax}^{CF_2}$ bands in the IR for C3F7-PHEMA suggests these groups in the bulk are not parallel to the substrate but randomly oriented.

Barrier Properties. We evaluated the effect of fluorination on the barrier properties of the PHEMA films using EIS upon exposure to 1 mM $K_3Fe(CN)_6$ and 1 mM $K_4Fe(CN)_6$ in 0.1 M Na_2SO_4(aq). Figure 4 contains the EIS spectra, in the form of Bode plots, for bare gold, the initiator-terminated monolayer, PHEMA, and the three fluorinated polymer films, all on gold. The solid curves in the plot represent best fits of the data with appropriate equivalent circuit models (Figure 5) to provide quantitative information on the effect of film composition on the resistance and capacitance of the films. For uncoated gold, the spectrum is fit with a model containing a solution resistance (R_s) in series with the following combination: Warburg impedance (Z_W) and charge-transfer resistance (R_{ct}) in series with one another but in parallel with a double-layer capacitance (C_{dl}).[43] The Warburg impedance that dominates this spectrum at low frequencies is consistent with rapid charge transfer between the redox probes and the

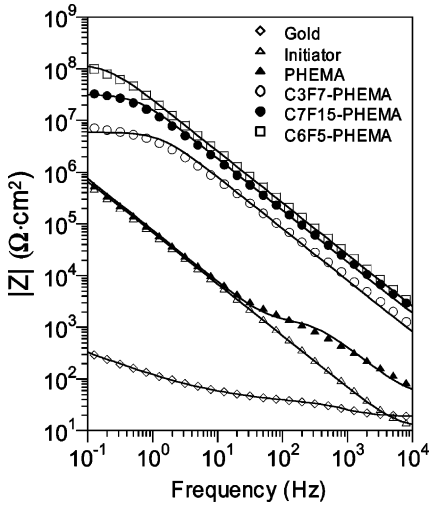

Figure 4. Electrochemical impedance spectra obtained in 1 mM $K_3Fe(CN)_6$ and 1 mM $K_4Fe(CN)_6$ in 0.1 M Na_2SO_4(aq) for films on gold. Spectra are shown for PHEMA before and after fluorination with bare gold and initiator-modified gold for reference. Solid curves represent fits of the data using appropriate equivalent circuit models.

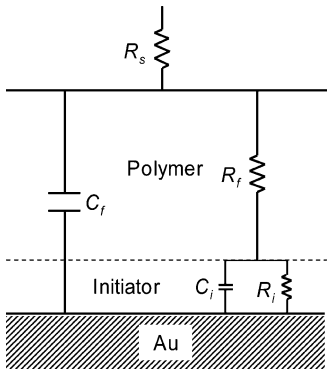

Figure 5. Equivalent circuit used to model impedance spectra for polymer films on gold. For PHEMA films on gold, both time constants (one due to initiator and one due to the polymer film) appear in the impedance spectrum. For fluorinated films, however, the impedance due to R_f is much greater than the combined impedance of R_i and C_i in parallel, so the time constant due to the initiator is not observed in the impedance spectra. For these cases, the equivalent circuit simplifies to a Randles model with R_f and C_f in parallel with one another but in series with R_s.

uncoated surface. The mere presence of the initiator monolayer on the gold surface dramatically increases the impedance and produces a spectrum that is fit with a parallel combination of initiator resistance (R_i) and capacitance (C_i) in series with R_s, identical in form to a Randles model equivalent circuit used previously to describe self-assembled monolayers.[44,45] Similar to the behavior of other types of monolayers on metal surfaces, this film blocks gold surface sites and greatly reduces charge transfer.

When a 270 nm thick film of PHEMA is grown atop the monolayer, the impedance spectrum in Figure 4 shows two time constants and is appropriately fitted with a more complex model (Figure 5) containing a polymer film resistance (R_f) and a total film (polymer plus initiator) capacitance (C_f). The time constant at low frequencies is caused by the initiator layer ($\tau_i = R_iC_i$) and is larger than that caused by PHEMA ($\tau_f = R_fC_f$). One surprising observation from Figure 4 is that growth of a ~270 nm film of PHEMA from the surface did not affect the impedance properties at low frequency as compared with those of the monolayer. This observation confirms that the contribution of PHEMA to the impedance spectrum is limited to the time constant at high frequencies. Table 3 enables comparison of the average capacitances and resistances for the initiator-terminated monolayer and PHEMA. Addition of the PHEMA layer reduces the total film capacitance (C_f) due to its enhanced thickness but exhibits a very low resistance (R_f) in comparison to that of the initiator (R_i). On a per unit thickness basis, SAMs generally provide much greater resistances than thin polymer films due to the minimization of defects during the monolayer assembly process.[46] The very low resistance of PHEMA indicates that it is loosely packed and a poor barrier film. This characteristic allows a larger molecule, namely a fluorinated acid chloride in our case, to effectively diffuse into the film and react with side chains throughout. If the PHEMA film were well-packed, acylation and film expansion would be unfavorable.

Table 3. Values for Initiator and Film Capacitance and Resistance in Fluorinated Polymer Films

sample	C_i (nF/cm²)	log R_i (Ω·cm²)	C_f (nF/cm²)	log R_f (Ω·cm²)
initiator	2400 ± 300	6.0 ± 0.4		
PHEMA	1900 ± 900	6.1 ± 0.5	640 ± 200	3.0 ± 0.3
C3F7-PHEMA			12 ± 7	6.7 ± 0.5
C7F15-PHEMA			9.2 ± 1.7	7.4 ± 0.4
C6F5-PHEMA			6.2 ± 0.7	7.8 ± 0.3

In contrast to the impedance behavior of PHEMA, fluorinated PHEMA films exhibit only one time constant. The key difference for the fluorinated films is that the time constant due to the initiator does not appear in the spectrum because R_f due to the fluorinated polymer is much greater than the combined impedance corresponding to R_i and C_i. Therefore, the equivalent circuit in Figure 5 simplifies to a Randles model in which R_s is in series with a parallel combination of R_f and C_f. Both R_i and C_i should remain relatively consistent throughout all polymer films although they could not be measured for the fluorinated films. Thus, for comparison purposes, only R_f and C_f values are compared between the different polymer films in Table 3.

In general, the best barrier films are those having the highest resistance and the lowest capacitance. Relating this idea to the impedance spectra in Figure 4, the films become progressively better barriers in going from the lowest curve (bare gold) to the highest curve (C6F5-PHEMA). Without exception, this trend shows increasing R_f and decreasing C_f as shown in Table 3. Comparison of R_f for C3F7-PHEMA with that for PHEMA shows a ~4 orders of magnitude improvement upon fluorination. Also, the film capacitance was lowered by a factor of ~50 due to the enhanced hydrophobicity of the partially fluorinated film that more effectively excludes water and yields a lower effective dielectric constant. For C7F15-PHEMA, the resistance was increased by a factor of 5 above C3F7-PHEMA with capacitance ~25% lower. The improved barrier performance of C7F15-PHEMA over C3F7-PHEMA is attributed to the higher fluorocarbon content and the ability of the longer fluoroalkyl chains to structure the film and minimize defects. The most surprising result from Figure 4 and Table 3 was that C6F5-PHEMA, even though the perfluorobenzoyl group was a short addition to the side chain, was actually the best barrier film studied, with the highest resistance and lowest capaci-

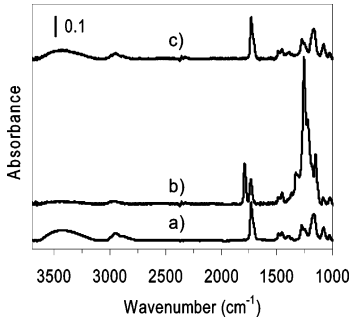

Figure 6. IR spectrum of a single PHEMA sample: (a) before fluorination, (b) after fluorination with $C_7F_{15}COCl$, and (c) after hydrolysis with 0.5 M KOH in ethanol for 1 min.

tance. This film provided an improvement over PHEMA by nearly 5 orders of magnitude for resistance and 2 orders of magnitude for capacitance. Even compared to the thicker C7F15-PHEMA film, C6F5-PHEMA exhibited a higher resistance (by a factor of 2.5) and a 30% lower capacitance. We attribute the superior protection of C6F5-PHEMA to the ability of the perfluoroaryl groups to exhibit dominant $\pi-\pi$ interactions, effectively stacking atop one another to structure the film and eliminate ion-conducting pathways. Fluoroaromatics like perfluorobenzene have been shown[28,47] to exhibit such strong $\pi-\pi$ interactions, even packing closer together than typical aromatic rings.

In summary, fluorinated side chains greatly improve barrier properties over PHEMA, most likely due to the structuring of the chains within the film, enhanced for longer perfluoroalkyl groups and for perfluoroaryl groups, and the water-repellent nature of the fluorocarbons that minimize water penetration. Merely taking up available space in the film does not account for the observed results, particularly when considering the resistance and capacitance of C6F5-PHEMA as compared with C7F15-PHEMA and C3F7-PHEMA.

Film Stability. In this work, the acylation reaction results in a fluorinated ester linkage on the polymer side chains. Esters having fluorocarbon constituency next to the carbonyl moiety are known to be susceptible to degradation upon exposure to heat[25,26] or base.[48] While gaining the surface properties of fluorinated polymers is directly advantageous for our method of surface-initiated polymerization and modification, the ability to simply and effectively cleave the fluorocarbon side chains could have a broad impact on the preparation of temporary resists or patterned films and surfaces.[25] The stability of PHEMA-based polymer films against hydrolysis was evaluated by placing samples of PHEMA, C3F7-PHEMA, C7F15-PHEMA, and C6F5-PHEMA in deionized water or a 0.5 M KOH solution in ethanol for various amounts of time, rinsing with deionized water, drying with nitrogen, and then examining their IR spectra. IR spectra for the samples exposed to water showed no detrimental effects even after 5 days of exposure. The PHEMA sample in KOH also showed no change in the IR spectrum. The IR spectra of the fluorinated polymers in KOH, on the other hand, show conversion of the film back to PHEMA within 1 min for the fluoroalkyl side chains (Figure 6) and within 30 min for the fluoroaryl side chain (not shown). Reversion to PHEMA was evidenced by the complete loss of the carbonyl peak at $\sim$1790 cm^{-1} and CF_2 stretching peaks, the regained peak in the hydroxyl region, and the regained intensity of the carbonyl at $\sim$1733 cm^{-1} (Figure 6). As previously mentioned, this last point provides confirmation that the original reduction in the carbonyl at 1733 cm^{-1} upon acylation was not due to chain loss but rather to orientational effects. Even the perfluorobenzoyl side chain, having no fluorine in the α-position, reverted back to PHEMA within 30 min as the ester was gradually hydrolyzed. These attributes are consistent with rapid hydrolysis of the fluorinated ester but an inability to hydrolyze the hydrocarbon PHEMA ester, which is much more stable.[48] The remarkable ability to convert these partially fluorinated polymer films back to PHEMA by simple immersion in base holds promise for the efficient patterning of polymer films and structures and may provide a new strategy to control the depth-dependent composition within polymer films.

Conclusions

Addition of fluorinated side groups to surface-initiated PHEMA through an acylation reaction results in a partially fluorinated polymer film and imparts desirable attributes such as hydrophobic and oleophobic surfaces and dramatically improved barrier properties. The acylation reaction alters film structure and results in a straightening of the polymer backbone and a resulting expansion of the film. A longer fluoroalkyl side group (C7F15) on PHEMA greatly improves the film properties in all areas—higher resistance, lower capacitance and critical surface tension, and better defined structure—as compared with a shorter fluoroalkyl chain (C3F7), most likely due to enhanced interchain interactions. A perfluoroaryl side group (C6F5) provides the greatest resistance and lowest capacitance of all the films, perhaps due to strong intermolecular stacking interactions of the fluoroaryl groups to greatly reduce ion-conducting paths. The production of fluorinated PHEMA in the manner described avoids many problems encountered with traditional fluorinated polymer films, such as solubility and adhesional issues, and enables rapid assessment of the role of side chain length and composition on film properties while maintaining a common reference film (PHEMA). Furthermore, the critical surface tensions of the fluoroalkyl-modified films are lower than those of PTFE and many other fluorinated polymers.

Acknowledgment. We gratefully acknowledge the National Science Foundation (CTS-0203183 and a NSF Graduate Research Fellowship (E.L.B.)) for financial support. We also thank Dr. Tomlinson Fort for allowing use of the contact angle goniometer and Dr. Bridget Rogers for use of the ellipsometer.

References and Notes

(1) Delucchi, M.; Turri, S.; Barbucci, A.; Bassi, M.; Novelli, S.; Cerisola, G. *J. Polym. Sci., Part B: Polym. Phys.* **2002**, *40*, 52−64.
(2) Wang, J. G.; Mao, G. P.; Ober, C. K.; Kramer, E. J. *Macromolecules* **1997**, *30*, 1906−1914.
(3) Tirelli, N.; Ahumada, O.; Suter, U. W.; Menzel, H.; Castelvetro, V. *Macromol. Chem. Phys.* **1998**, *199*, 2425−2431.
(4) Sivakumar, C.; Wen, T. C.; Gopalan, A.; Teng, H. *Synth. Met.* **2003**, *132*, 219−226.
(5) Fukushima, H.; Seki, S.; Nishikawa, T.; Takiguchi, H.; Tamada, K.; Abe, K.; Colorado, R.; Graupe, M.; Shmakova, O. E.; Lee, T. R. *J. Phys. Chem. B* **2000**, *104*, 7417−7423.
(6) Mackie, N. M.; Castner, D. G.; Fisher, E. R. *Langmuir* **1998**, *14*, 1227−1235.
(7) Lau, K. K. S.; Murthy, S. K.; Lewis, H. G. P.; Caulfield, J. A.; Gleason, K. K. *J. Fluorine Chem.* **2003**, *122*, 93−96.

(8) Jung, D. H.; Park, I. J.; Choi, Y. K.; Lee, S. B.; Park, H. S.; Ruhe, J. *Langmuir* **2002**, *18*, 6133−6139.
(9) Li, K.; Wu, P. P.; Han, Z. W. *Polymer* **2002**, *43*, 4079−4086.
(10) Lovinger, A. J. *Sci. Am.* **2002**, *286*, 100.
(11) Matyjaszewski, K. *Macromol. Symp.* **2001**, *174*, 51−67.
(12) Boyes, S. G.; Brittain, W. J.; Weng, X.; Cheng, S. Z. D. *Macromolecules* **2002**, *35*, 4960−4967.
(13) Prucker, O.; Ruhe, J. *Macromolecules* **1998**, *31*, 592−601.
(14) Kim, J. B.; Huang, W. X.; Miller, M. D.; Baker, G. L.; Bruening, M. L. *J. Polym. Sci., Polym. Chem.* **2003**, *41*, 386−394.
(15) Wang, J. S.; Matyjaszewski, K. *J. Am. Chem. Soc.* **1995**, *117*, 5614−5615.
(16) Kato, M.; Kamigaito, M.; Sawamoto, M.; Higashimura, T. *Macromolecules* **1995**, *28*, 1721−1723.
(17) Matyjaszewski, K.; Miller, P. J.; Shukla, N.; Immaraporn, B.; Gelman, A.; Luokala, B. B.; Siclovan, T. M.; Kickelbick, G.; Vallant, T.; Hoffmann, H.; Pakula, T. *Macromolecules* **1999**, *32*, 8716−8724.
(18) Wang, X. S.; Lascelles, S. F.; Jackson, R. A.; Armes, S. P. *Chem. Commun.* **1999**, 1817−1818.
(19) Wang, X. S.; Jackson, R. A.; Armes, S. P. *Macromolecules* **2000**, *33*, 255−257.
(20) Wang, X. S.; Armes, S. P. *Macromolecules* **2000**, *33*, 6640−6647.
(21) Robinson, K. L.; Khan, M. A.; Banez, M. V. D.; Wang, X. S.; Armes, S. P. *Macromolecules* **2001**, *34*, 3155−3158.
(22) Huang, W. X.; Kim, J. B.; Bruening, M. L.; Baker, G. L. *Macromolecules* **2002**, *35*, 1175−1179.
(23) Shah, R. R.; Merreceyes, D.; Husemann, M.; Rees, I.; Abbott, N. L.; Hawker, C. J.; Hedrick, J. L. *Macromolecules* **2000**, *33*, 597−605.
(24) Gopireddy, D.; Husson, S. M. *Macromolecules* **2002**, *35*, 4218−4221.
(25) Boker, A.; Reihs, K.; Wang, J. G.; Stadler, R.; Ober, C. K. *Macromolecules* **2000**, *33*, 1310−1320.
(26) Boker, A.; Herweg, T.; Reihs, K. *Macromolecules* **2002**, *35*, 4929−4937.
(27) Sandrin, L.; Silverstein, M. S.; Sacher, E. *Polymer* **2001**, *42*, 3761−3769.
(28) Adams, N.; Cowley, A. R.; Dubberley, S. R.; Sealey, A. J.; Skinner, M. E. G.; Mountford, P. *Chem. Commun.* **2001**, 2738−2739.
(29) Nuzzo, R. G.; Dubois, L. H.; Allara, D. L. *J. Am. Chem. Soc.* **1990**, *112*, 558−569.
(30) Coleman, M. M.; Lee, K. H.; Skrovanek, D. J.; Painter, P. C. *Macromolecules* **1986**, *19*, 2149−2157.
(31) Silverstein, R. M.; Webster, F. X. *Spectrometric Identification of Organic Compounds*, 6th ed.; Wiley: New York, 1998.
(32) Tsao, M. W.; Hoffmann, C. L.; Rabolt, J. F.; Johnson, H. E.; Castner, D. G.; Erdelen, C.; Ringsdorf, H. *Langmuir* **1997**, *13*, 4317−4322.
(33) Parikh, A. N.; Allara, D. L. *J. Chem. Phys.* **1992**, *96*, 927−945.
(34) Han, L. C. M.; Timmons, R. B.; Lee, W. W.; Chen, Y. Y.; Hu, Z. B. *J. Appl. Phys.* **1998**, *84*, 439−444.
(35) Naud, C.; Calas, P.; Commeyras, A. *Langmuir* **2001**, *17*, 4851−4857.
(36) Levitt, M.; Perutz, M. F. *J. Mol. Biol.* **1988**, *201*, 751−754.
(37) Laibinis, P. E.; Palmer, B. J.; Lee, S.-W.; Jennings, G. K. Self-Assembled Monolayers of Thiols. In *Thin Films*; Ulman, A., Powell, R., Francombe, M. H., Eds.; Academic Press: New York, 1998; Vol. 24 and references therein.
(38) Weinstein, R. D.; Moriarty, J.; Cushnie, E.; Colorado, R.; Lee, T. R.; Patel, M.; Alesi, W. R.; Jennings, G. K. *J. Phys. Chem. B* **2003**, *107*, 11626−11632.
(39) de Boer, B.; Meng, H.; Perepichka, D. F.; Zheng, J.; Frank, M. M.; Chabal, Y. J.; Bao, Z. N. *Langmuir* **2003**, *19*, 4272−4284.
(40) Zisman, W. A. *Contact Angle, Wettability, and Adhesion*; American Chemical Society: Washington, DC, 1964; Vol. 43.
(41) Bin Zhang, Z.; Ying, S. K.; Hu, Q. H.; Xu, X. D. *J. Appl. Polym. Sci.* **2002**, *83*, 2625−2633.
(42) Genzer, J.; Sivaniah, E.; Kramer, E. J.; Wang, J. G.; Korner, H.; Xiang, M. L.; Char, K.; Ober, C. K.; DeKoven, B. M.; Bubeck, R. A.; Chaudhury, M. K.; Sambasivan, S.; Fischer, D. A. *Macromolecules* **2000**, *33*, 1882−1887.
(43) Janek, R. P.; Fawcett, W. R.; Ulman, A. *Langmuir* **1998**, *14*, 3011−3018.
(44) Jennings, G. K.; Munro, J. C.; Yong, T. H.; Laibinis, P. E. *Langmuir* **1998**, *14*, 6130−6139.
(45) Yan, D.; Saunders, J. A.; Jennings, G. K. *Langmuir* **2000**, *16*, 7562−7565.
(46) Jennings, G. K.; Munro, J. C.; Laibinis, P. E. *Adv. Mater.* **1999**, *11*, 1000−1003.
(47) Lorenzo, S.; Lewis, G. R.; Dance, I. *New J. Chem.* **2000**, *24*, 295−304.
(48) Tonelli, C.; Di Meo, A.; Barchiesi, E. *J. Polym. Sci., Polym. Chem.* **2002**, *40*, 4266−4280.

MA035471V